Study of Thermocurrents in ILC cavities via measurements of the Seebeck Effect in niobium, titanium, and stainless steel thermocouples

Victoria Cooley

Chemistry Department, University of Wisconsin-Madison

Madison, WI 53706

Supervisor: Anthony C. Crawford

Cavity Processing R&D, Technical Division

Fermi National Accelerator Laboratory

Batavia, IL 60510

2014 Summer Undergraduate Internship

Abstract

The goals of Fermilab's Superconductivity and Radio Frequency Development Department are to engineer, fabricate, and improve superconducting radio frequency (SCRF) cavities in the interest of advancing accelerator technology. Improvement includes exploring possible limitations on cavity performance and mitigating such impediments. This report focuses on investigating and measuring the Seebeck Effect observed in cavity constituents titanium, niobium, and stainless steel arranged in thermocouples. These junctions exist between cavities, helium jackets, and bellows, and their connection can produce a loop of electrical current and magnetic flux spontaneously during cooling. The experimental procedure and results are described and analyzed. Implications relating the results to cavity performance are discussed.

Keywords: Superconducting RF cavities, Seebeck Effect, thermocouple, titanium helium vessel

1. Introduction

SCRF cavities are the primary type of cavity being applied in high-energy accelerators, such as the Linear Coherent Light Source-II and the European X-ray Free Electron Laser. Cavity research at Fermilab has been paramount in developing and continually improving these cavities. Of particular interest at Fermilab is the nine-cell niobium radio-frequency cavity. The cavity is made mostly of high-purity niobium, although a titanium-niobium alloy exists at either end. A cylindrical titanium jacket is welded to these titanium-niobium ends so that it completely encases the cavity. The titanium jacket features titanium bellows which are significantly thinner than the rest of the jacket. The jacket acts as a helium vessel when the cavity is cooled to superconducting temperatures. Figure 1 shows basic diagrams and dimensions of a nine-cell cavity. Throughout this report, green represents titanium and grey represents niobium.

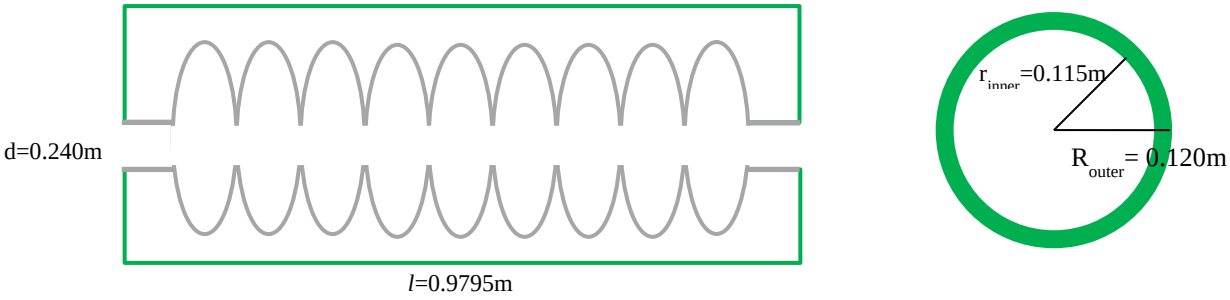

Figure 1 Niobium cavity and titanium helium vessel geometry and dimensions

For peak performance, niobium SCRF cavities need careful magnetic shielding. Magnetic field lines around the cavity's inside surface dissipate energy when radio-frequency current is applied. Energy dissipation as a result of magnetic field lines around the cavity lowers the quality of the cavity. The quality factor (Q) of a cavity is a ratio of energy stored to energy dissipated per resonance cycle [1]; a large Q, on the order of 10^{10} or 10^{11}, is desired in cavity operations because it is, therefore, directly coupled to the cryogenic heat loss.

Because cavities are shielded from external magnetic fields, internal magnetic fields generated by current loops around a cavity-helium vessel circuit are a primary concern. This current may arise during the cooling process. To become superconducting, a niobium cavity must be cooled to below the material's critical temperature T_c, which is approximately 9.2 K for high purity niobium. Liquid helium (LHe) is used to reach these low temperatures. During the cooling process, it is possible to create a thermal gradient by cooling the cavity too rapidly or too unevenly. If the thermal gradient is sufficient enough, it is possible to generate an electric current via a phenomenon known as the Seebeck Effect.

Figure 2 Diagram of a thermocouple

The Seebeck Effect in thermocouple circuits like the helium vessel-cavity system being studied occurs when a system of dissimilar metals is exposed to a thermal gradient in which the junction of the two metals is a different temperature than the other end of the system (Figure 2). To explain why this occurs, the electrons and holes in a thermoelectric material are described as behaving like a gas with charged particles [2]. If a gas is sealed in a container with a hot region and a cold region, the gas molecules will move faster at the hot end and diffuse faster than the cold molecules such that a net build of molecules will be present at the cold end. Because these molecules carry charge, there will be a resulting electrostatic force that repels the molecules at the cold end and drive them back to the hot end.

In the case of thermoelectric materials, the potential generated by the buildup of charge at the cold end causes current to flow through the circuit, provided the materials are electrically connected. The temperature difference between the ends of the thermocouple produces the potential, or voltage, and the heat flow along the thermocouple facilitates the current. An equivalent circuit

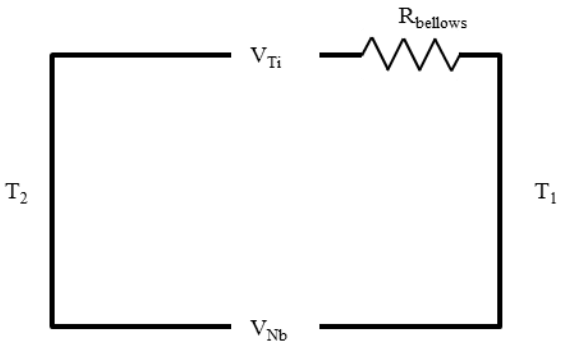

Figure 3 Equivalent circuit of a cavity-vessel thermocouple

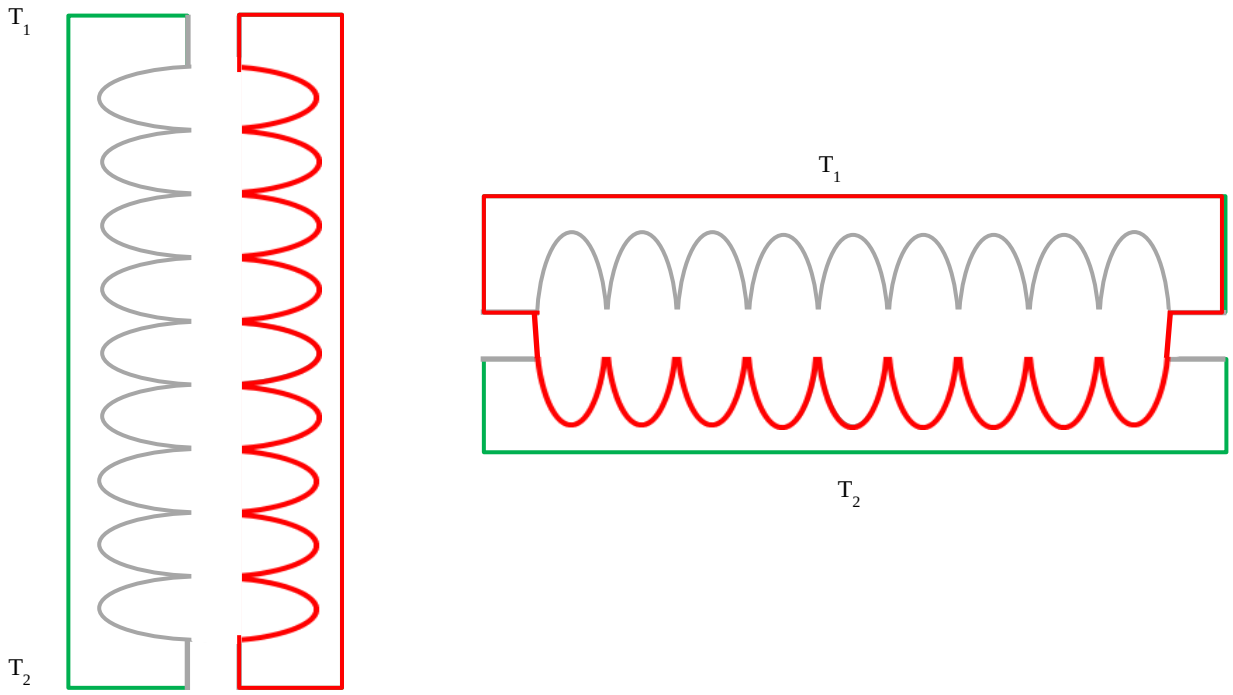

Figure 4a (left) a vertical orientation of cavity during cool down; 4b (right) a horizontal orientation during cool-down (theoretical, unconfirmed); 4c (below) strength of magnetic field as a function of distance from center line of cavity [3]

of a cavity-helium vessel thermocouple that follows the principles of the Seebeck Effect is simple in design (Figure 3).

Two possible current loops (Figure 4a, b) may result from different orientations of the cavity-helium vessel system curing cool-down. The current in Figure 4a, which flows around half of the cavity-helium vessel system, can result from cool-down in the vertical position. As helium pools around the

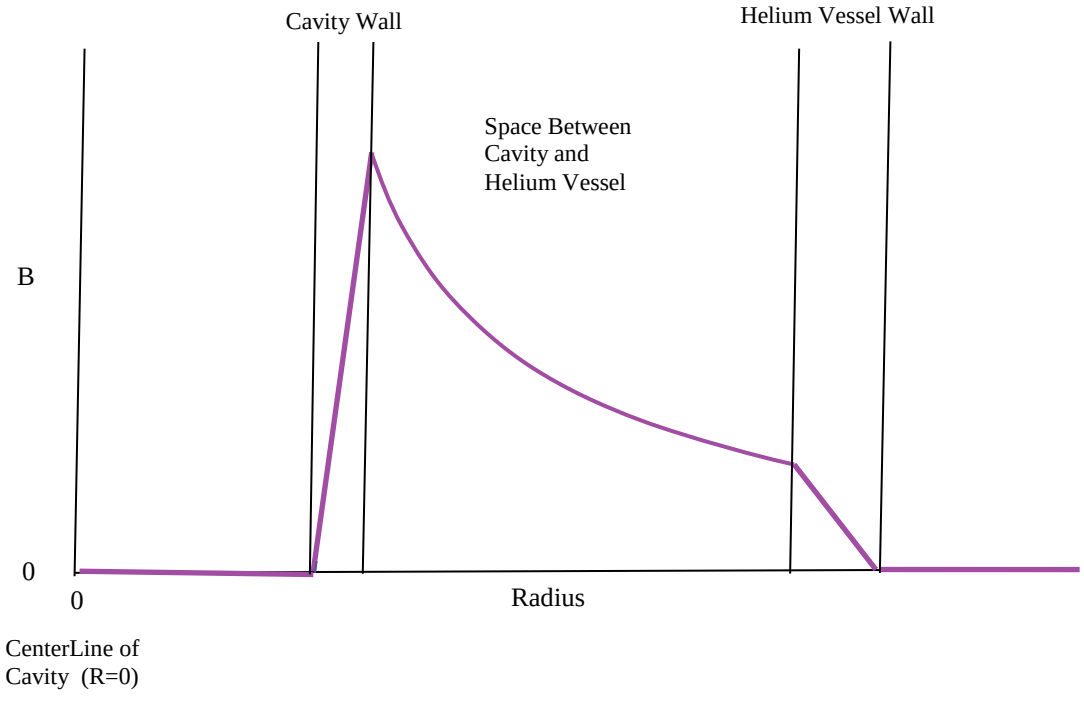

bottom of the system, the thermal gradient becomes established along the length of the cavity. The resulting current path creates a magnetic field that does not penetrate into the interior of the cavity itself, but rather exists only at radii larger than the inside cavity wall (Figure 4c). In this scenario, only the trapped magnetic flux in the interior wall of the cavity is relevant to Q degradation [4].

If the cavity is oriented in a horizontal position during cool down, a current like the one shown in Figure 4b is thought to result, although this has never been confirmed. When the cavity is cooled horizontally, the helium collects between the walls of the niobium and the titanium helium vessel on the bottom of the system. Only the bottom half of the cavity is cooled and thus becomes superconducting with a significantly reduced resistivity. Instead of flowing around half of the system, the current tends towards a path of least resistance, which includes the bottom of the cavity. This current path allows for the possibility of magnetic penetration into the cavity; therefore, trapped magnetic flux at radii greater than the inner wall of the cavity may be considered as sources of Q degradation.

The mechanism by which niobium becomes superconducting is complex and has yet to be fully understood by scientists. Cool-down is a dynamic process with many nuances that relate to Q depression; therefore, a more comprehensive analysis of internal magnetic field strength, not covered in this report, is necessary to determine the precise correlation of current loops to Q degradation.

This report will focus only on studying the Seebeck Effect as it applies to niobium stainless steel (Nb+SS) and niobium titanium (Nb+Ti) thermocouples and determining the magnitude of current it is possible to create. These materials were chosen to represent the niobium cavity and its surrounding helium vessel. Although titanium is a typical metal for helium vessels and the material of interest in this report, stainless steel is another possible helium vessel constituent. Experiment 1 focused on establishing a base-line potential measurement across a maximum thermal gradient to compare with theoretical data and to design further experiments. Experiment 2 was carried out to confirm the results of experiment 1. Finally, the purpose of experiment 3 was to measure the Seebeck Effect over a range of thermal differentials and to explore possible sources of error.

2. Procedures

The principle behind observing the Seebeck effect in a thermocouple is simple: if the thermocouple junction is held at a different temperature than the thermocouple leads are, a measurable potential will result. In this series of experiments, a temperature gradient is established by immersing the junction in a cryogenic coolant and holding the leads at a warmer temperature. The following sections describe the equipment used and major procedures carried out. For minor procedures, refer to Appendix A.

2.1 Cryogenic coolants

Common coolants for thermocouple experiments include liquid nitrogen (77 K) and liquid helium (4.2 K). For this series of experiments, a 60-L Dewar of liquid helium was used. While the temperature of the liquid may be considered constant at 4.2 K, a range of temperatures is present in strata of gaseous helium above the liquid. In all experiments, the junctions of the thermocouples were submerged in the liquid helium. The gradient of temperatures in the Dewar facilitated gradually cooling the leads during experiment 3 (section 2.6), which allowed for multiple measurements over several temperatures. The equipment of experiment 3 prompted the removal of the Dewar neck. The larger opening was sealed by a ceramic ring cut to fit the Dewar's O-ring, secured with the Dewar neck clamp, and sealed in the center with excess plumber's putty when not in use.

2.2 Nanovoltmeter

To measure the voltage along a thermocouple circuit in a temperature gradient of less than 300 K, it is imperative to use a voltmeter that can detect signal fluctuations as small as tenths or hundredths of microvolts. For this reason, a Keithley 2182A nanovoltmeter was utilized. To accommodate small readings, low-level voltage detection techniques suggested by the manufacturer were applied, including calculating corrected voltages (Appendix C) and connecting the thermocouple to the voltmeter with twisted or coaxial leads [5]. A digital filter was programed into the nanovoltmeter for all experiments carried out (Appendix A).

2.3 Resistance Temperature Detector (RTD)

Experiment 3 required measuring the temperature of the thermocouple leads as they were lowered into the various temperature strata of helium gas in the Dewar. Therefore, a Lake Shore Cernox™ RTD was mounted and inserted into the Dewar with the thermocouple leads. The RTD was connected to a Lake Shore digital box and was calibrated using Lake Shore calibration curve software prior to experimentation.

2.4 Experiment 1: Sampling Seebeck effect at 4.2 K and 300 K in Nb+Ti and Nb+SS thermocouple circuits

The thermocouple leads were twisted with tin-coated copper coaxial leads to form a connection. To prevent excess fluctuations from air currents in the room, the junction of the thermocouple was secured at room temperature with a rubber shroud around it such that the shroud did not make contact with the junction. Once the thermocouple circuit appeared to reach thermal equilibrium, a voltage was recorded manually. The junction was then immersed in LHe without the shroud while the leads remained at room temperature. A voltage was recorded manually once thermal equilibrium was reached. The thermocouple was then removed, the sources reversed and re-twisted, and the procedure was repeated. Both the Nb+Ti and Nb+SS thermocouples were tested.

2.5 Experiment 2: Sampling Seebeck effect at 4.2 and 300 K in Cu reference thermocouple circuits

Cu+Ti, Cu+Nb, and Cu+SS thermocouples were fashioned (Appendix A). The thermocouple leads were twisted with tin-coated copper coaxial voltmeter leads. The thermocouple was secured with a rubber shroud at room temperature, and a voltage was recorded manually. The junction was then immersed in LHe without the shroud and a second measurement was made manually. The thermocouple was removed, the sources were reversed and re-twisted, and the procedure was repeated for the reversed sources. All three thermocouples were tested.

2.6 Experiment 3: Measuring Seebeck effect along a thermal gradient at leads in Nb+Ti and Nb+SS thermocouple circuits

An RTD was mounted on a copper support and inserted into the end of a five-foot metal support rod, such that the wiring connecting the RTD ran the length of the rod to the Lake Shore connector box

and exited the other end. The leads of the thermocouple were secured to the end of the support rod with Kapton tape. The leads were twisted with tin-coated copper coaxial voltmeter leads, which were also secured to the support rod with Kapton tape, at the same position of the RTD to ensure accurate lead temperature measurements. The length of the thermocouple was allowed to hang freely from the end of the rod.

Using a length of rope attached to the top end of the support rod and looped over a support beam to create a crude pulley system, the support rod was raised above the Dewar and lowered into the enlarged opening created by the ceramic ring (section 2.1). The support rod was lowered until heavy evaporation leaving the Dewar indicated that the junction had been immersed in LHe. Manual data acquisition began and continued as the support rod was slowly lowered into the Dewar. Temperature and corresponding voltage were recorded for each height. Data acquisition ended when the leads had been lowered to the surface of the liquid.

Because the junction end of the thermocouple was pushed further into the liquid and likely against the bottom of the Dewar, it was bent and put under stress. To remove the thermocouple without causing significant damage to the junction end, the support rod was slowly lifted out of the Dewar, allowing the thermocouple to thaw gradually. The procedure was repeated multiple times with both thermocouples subjected to several key variations. The variations are summarized in Table 2.

Table 2 Experiment 3 Variations

Trial Number, Thermocouple Identity	**Variation of Experiment 3**
Trial 1 Nb+Ti	Procedure as written; measurements made raising and lowering lead temperature
Trial 2 Nb+Ti	Procedure as written; measurements made lowering lead temperature only
Trial 3 Nb+Ti	Twisted lead connections replaced with copper alligator clip connections and leads
Trial 4 Nb+SS	Procedure as written; measurements made lowering lead temperature only
Trial 5 Nb+SS	Twisted lead connections replaced with copper alligator clip connections and leads

3. Results and Discussion

Table 3 Experiment 1: Seebeck Voltages in Nb Thermocouples, sampled at 4.2K and at room temperature

Condition of Junction	Nb+Stainless Thermocouple	Nb+Ti Thermocouple
Room temp., no shroud	N/A	3.2-4.0 μV
Room temp., shroud	.017 μV	4.0-4.5 μV
Room temp., shroud, reversed sources	-0.05 μV	2.0 μV
4.2 K	-0.51 mV	-0.45 mV
4.2 K, reversed sources	0.50 mV	0.45 mV

3.1 Experiment 1 Discussion: Stability

The voltmeter's digital filter helped to give more stable measurements with fewer erratic fluctuations than those measurements made without the filter; however, they were still somewhat erratic, especially at room temperature without the rubber shroud. It is unknown precisely why the rubber shroud further stabilized measurements, but perhaps the shroud helped protect the junction from air currents that could alter the temperature slightly. When both the shroud and filter were applied, and thermal equilibrium was reached, readings tended to "bounce" between constraints that slowly narrowed as measurement continued. To accommodate for this inevitable fluctuation, at least three cycles of "bouncing" were allowed to occur before a window of measurement was considered small enough to take a reading for each measurement.

Readings fluctuated much less when the junction was immersed in LHe. This might be the case because the temperature of the junction is more constant in LHe than it is in the air. Additionally, the voltages at room temperature are on the order of microvolts. Because they are so small, they are likely to appear to fluctuate greatly. The voltages observed at a junction temperature of 4.2 K are on the order of millivolts; the readings still fluctuated at by a tenth of a microvolt, but appeared steady because the measurement was now accurate to three decimal places instead of one.

Measurements of the Nb+SS sample were much steadier at both temperatures than those observed using the Nb+Ti sample in that initial fluctuations were smaller and slower. Because both samples were

subjected to identical conditions, this is most likely due to the properties of the constituent metals themselves.

Table 4 Experiment 2: Seebeck Voltages in Cu Thermocouples, sampled at 4.2 K and room temperature

Condition of Junction	Cu+SS	Cu+Nb	Cu+Ti
Room temp., shroud	2.3 μV	2.1 μV	1.3 μV
Room temp., shroud, reversed sources	-2.4 μV	-1.6 μV	-1.3 μV
4.2 K	-0.50 mV	-0.012 mV	-0.46 mV
4.2 K, reversed sources	0.51 mV	0.013 mV	0.46 mV

3.2 Experiment 2 Discussion: Connection and Low-Voltage Detection Techniques

Low-voltage detection techniques were applied in experiment 2. The primary technique tested was twisting the thermocouple along the length of the wires to limit magnetic interference (Appendix A). Unfortunately, there was no apparent effect on the voltages recorded, which were still quite erratic at room temperature and more stable at low junction temperature. There appeared to be no advantage to applying this technique.

There may be concern about the connections between the individual wires in the thermocouples. The junctions were formed by twisted wires secured with shrink tubing instead of by spot welds. Because the contact methods were different between experiments, the connections used in this experiment present a possible source for significant error between experimental data sets themselves and between theoretical and experimental data. The twisted connection between the thermocouple wires is less secure than the welded junction of the niobium thermocouple circuits, allows for the formation of oxides on the surfaces connecting the two wires, and introduces many points of contact between the wires, which may produce multiple circuits.

The measurements obtained in experiment 1 and experiment 2 differ by an average of 17%. Because the purpose of experiment 2 was merely to confirm the measurements recorded in experiment 1 and to explore low-voltage detection techniques, an average error of 17% is small enough in regards to the large gap between theoretical and experimental data, discussed below, to confirm the data obtained in experiment 1 despite the poor connections between thermocouple wires.

Table 5 Comparing Experimental and Theoretical Seebeck Voltages, Experiments 1 and 2

	Nb+SS, Room temp.	Nb+SS, 4.2 K	Nb+Ti, Room temp.	Nb+Ti, 4.2 K
Corrected Voltage, Exp. 1	0.314 μV	0.51 mV	1.1 μV	0.45 mV
Corrected Voltage, Exp. 2	0.5 μV	0.50 mV	1.2 μV	0.45 mV
Theoretical Voltage	N/A	N/A	0 μV	0.25 mV

3.3 Experiments 1 and 2 Discussion: Comparing to Theoretical Data

The data obtained for the Nb+Ti thermocouple circuit did not agree with theoretical data calculated by using a best-fit model of absolute Seebeck coefficients (Appendix C). Unfortunately, no data was available for the Seebeck coefficients of stainless steel. The following discussions on theoretical data and error pertain to the Nb+Ti sample only, although some experimentation on the Nb+SS sample offered further insights into data reproducibility.

By subtracting the voltages from two copper thermocouples, it is possible to effectively cancel out the Seebeck effect in copper, thus giving a second set of readings for the niobium thermocouples (Appendix C). To compare Nb+Ti voltages between experiments or between experimental and theoretical, corrected voltages are used [6]. These corrected voltages are computed as the average of the difference between reversed source measurements (Appendix C). When the Seebeck effect of copper is mathematically canceled out and the corrected voltages compared, the voltages of experiment 1, which are confirmed by experiment 2, differ with corresponding theoretical voltages by over 100%, or 0.24 mV. Possible sources of error include contamination in the form of surface oxides or impure wires that will produce different voltages than the theoretical data, which is calculated for pure wires only; poor connection between the voltmeter and thermocouple leads, which are merely twisted together; excess background noise that may interfere with the measurement of the voltages; and the thermocouple junction not being fully immersed in liquid helium, which would set different endpoints on the calculation of the theoretical data. Many of these potential sources of error were tested in experiment 3 and its variations.

Figure 5. Comparing Voltages in Nb+Ti Thermocouple Circuit in Thermal Gradient

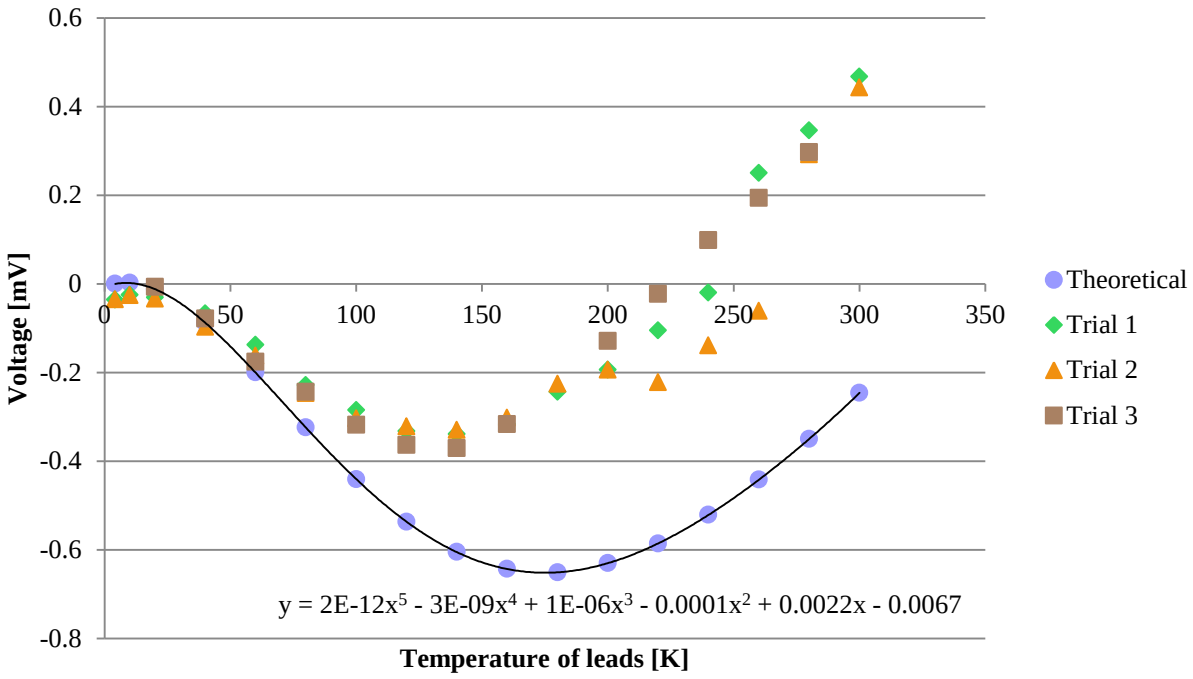

Figure 6. Comparing Voltages in Nb+SS Thermocouple Circuit in Thermal Gradient

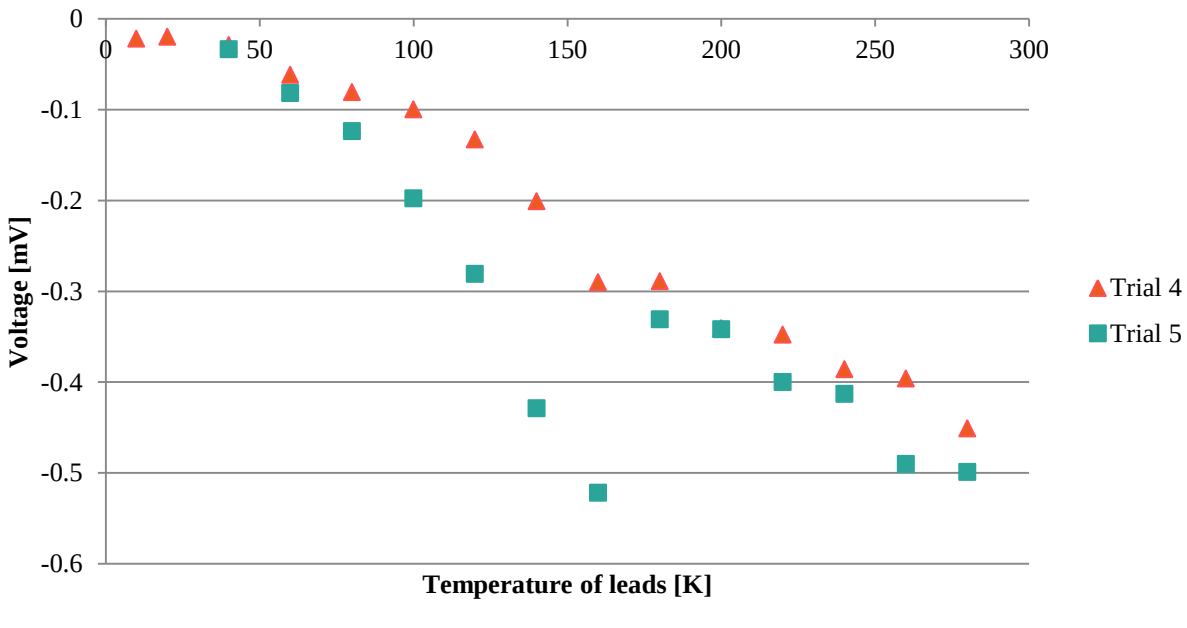

3.4 Experiment 3 Discussion: Comparing to Theoretical Data and Sources of Error

In Trials 1 and 2, the data appeared reasonably reproducible. Results such as these that are precise compared with each other but inaccurate compared to theoretical suggest a systematic error in the experimental process. These errors include those discussed previously (3.3) as well as circuit interference from the voltmeter leads, which were exposed to the thermal gradient and assumed to generate no voltage along the circuit.

The significant difference between theoretical and experimental data for the Nb+Ti thermocouple circuit, confirmed in all three experiments, prompted a series of trials to determine the sources of error responsible.

Trials 3 and 5 aimed to determine any difference between a twisted lead connection and a spring-tension connection. Alligator clip connections replaced twisted lead connections in Trials 3 and 5, and the data that was produced differed from previous trials by an average of 37% or by 50 μV—a margin that does not account for the 600 μV gap between the theoretical and experimental data. Poor connection between the leads can thus be ruled out.

The twisted lead short circuit test produced voltages not exceeding a magnitude of 25 μV; it can therefore be concluded that the voltage generated by the thermal gradient along the leads, while not zero as previously assumed, is not large enough to account for the significant variation between experimental and theoretical.

Unlike the twisted lead short circuit test, which produced a pattern of voltages vs. temperature that can easily be modeled (Appendix B), the alligator clip short circuit test produced seemingly random data that could not be correlated by any best-fit model. Because the data was imprecise, random error is most likely responsible for the erratic readings. A likely source of random error is background noise interfering with the wires, which were neither coaxial nor shielded with a metal casing. It is highly unlikely that this random error, which did not exceed 50 μV at any temperature, produced a systematic error of up to 600 μV in the experimental data. Interference from the alligator clip-connected leads being

exposed to a thermal gradient is not solely responsible for the disparity between theoretical and experimental.

Another source of error considered is not immersing the junction completely in LHe. One way to remove this error is to mount a second RTD at the thermocouple junction to precisely measure its temperature and ensure its immersion. Regrettably, the setup used in experiment 3 does not allow for the inclusion of two RTDs. Redesigning the experiment is impractical if other methods can be used to confirm the junction's immersion. For example, careful monitoring of the level of helium in the Dewar and dislodging any obstructions like ice blocks can ensure the thermocouple is long enough and has a clear path to make it to the liquid's surface.

In any case, a variation of several Kelvin at the thermocouple junction would not account for the disparity between the data. Variations of about 1 K around 4.2 K correspond to an error of less 1 μV overall based on the theoretical model.

Once all extrinsic sources of error are exhausted, it is necessary to consider intrinsic sources of error present in the sample of wire tested. The exact conditions of samples used to obtain the absolute Seebeck coefficients of niobium and titanium and thus the theoretical data examined are unknown. It is assumed that the samples were annealed and of high purity. The constituent wires used in this series of experiment were handled quite extensively, which caused bending and stressing in the wire structure. The stressed condition of the wires may have affected the Seebeck voltages observed. In addition, there is potential for impurities in the experimental samples, which similarly affect the voltage generated.

3.5 Implications

The degree to which the Seebeck Effect generates a current sufficient enough to produce appreciable amounts of trapped magnetic flux depends primarily on the size of the thermal gradient. The currents calculated in Table 6 follow parameters listed in

Approximate Temperature Differential (K)	Average Electrical Potential (mV)	Current (A)
0	0.024	0.822
5	0.026	0.890
10	0.014	0.479
15	0.024	0.822
25	0.042	1.44
35	0.080	2.74
45	0.121	4.14

Table 6 Voltages observed in Nb+Ti thermocouple as a function of temperature differential

[4] as well as those given in Figure 1 to approximate total resistance along a cavity-helium vessel circuit as 2.92×10^{-5} Ω.

It is important to stress that any flux created by the Seebeck effect is an internal source, which is not possible to shield by the various layers of magnetic material surrounding cavity test pits or cryomodules. The orientation of the cavity during cool-down plays a large role in determining where the magnetic field may be present, although further complication may arise when various regions experience the Meissner Effect and impose motion of flux onto other, warmer, regions.

4. Conclusion

We successfully measured and verified the magnitude of potentials possible by the Seebeck Effect along niobium stainless steel and niobium titanium thermocouples when they are subjected to a thermal gradient. The Seebeck coefficients obtained from the data followed theoretical trends, but with offsets at temperature above ~50 K. For either thermocouple, substantial voltages were reproduced by multiple measuring techniques. We determined that at 50 K (a gradient of 45 K), an electrical potential of 4.14 A was produced. Information about other factors in the cool-down process is needed to make sound conclusions about the influence of this current on cavity quality and performance.

5. References

1. Koech, J. C., "Cryomodule Magnetic Field Measurements", Fermi National Accelerator Laboratory, 2010.

2. Snyder, G. J., E. S. Toberer, "Complex Thermoelectric Materials", *Nature Materials 7*, 2008, p. 105-107.

3. Crawford, A. C., "Thermocurrent Induced Magnetic Fields in ILC Cavities", Fermi National Accelerator Laboratory, 17 July 2014.

4. Crawford, A. C., "A Study of Induced Magnetic Fields in ILC Cavities", Fermi National Accelerator Laboratory.

5. Daire, A., “Low-Voltage Measurement Techniques”, Keithley Instruments, Inc., 2005.

6. “Making Precision Low Voltage and Low Resistance Measurements”, Keithley Instruments, Inc., 2013.

7. “Model 3182A Specifications”, Keithley Instruments, Inc., p. 5.

8. “Cernox™ RTDs”, Lake Shore Cryotronics, Inc., p. 44.

6. Acknowledgements

I would like to thank my supervisor, Curtis Crawford, and advisor, Lance Cooley, for their guidance and incredible help during my time here at Fermilab. I would also like to extend my gratitude to Rob Schuessler for his extensive support in the lab and to Chuck Grimm for providing useful information. Further thanks go to all employees of the Technical Division and to Fermilab for providing this memorable opportunity.

Appendix A: Minor Procedures

A.1 Preparation of thermocouples

Each thermocouple was formed by spot welding niobium wire to either titanium or stainless steel wire. Once welded, each wire was insulated in rubber shrink tubing, leaving the junction and leads exposed. Each pair was then insulated in a wider piece of shrink tubing, again leaving the ends exposed.

A.2 Preparation of Copper reference thermocouples

Lengths of copper, niobium, titanium, and stainless steel wire were cut and insulated individually with shrink tubing. To form the Cu+Nb and Cu+Ti thermocouple, the lengths of the wires were taped parallel to each other using Kapton tape and the exposed ends twisted together and secured with a piece of shrink tubing. The copper wire was reused for all three thermocouples. To form the Cu+SS thermocouple, the

Table A1 Constituent wire specifications

Wire Material	Specifications	Supplier
Niobium	0.25 mm diameter, 99.9% pure, annealed	Goodfellow Specialty Metals
Titanium	0.25 mm diameter, 99.6+% pure, annealed	Goodfellow Specialty Metals
Copper	16-oz., oxygen-free electrolyte grade	Fermilab supply room
Stainless steel	0.25 mm diameter, 316L, temper as drawn	Goodfellow Specialty Metals

lengths of the wires were twisted together and secured with Kapton tape. The junction was formed by twisting the exposed ends together and securing with shrink tubing.

A.3 Setting up Keithley 2182A nanovoltmeter digital filters

For experiments 1 and 2, a 100-count, 10% window, moving target filter was applied using instructions from Keithley appropriate for the 2182A model. This filter keeps 100 measurements in a stack; each new measurement replaces the oldest one in the stack. If a measurement does not lie within 10% of the stack reading, a new stack is taken up.

For experiment 3, a 10-count, 1% window, repeating average filter was applied. This filer has a stack size of 10 readings, each within 1% of the stack reading. Ten new readings replace each stack before a new reading is shown.

A.4 Twisted lead short circuit test

The coaxial, tin-coated copper voltage leads were twisted together, mounted to the support rod at the same height as the RTD and slowly lowered into the Dewar. The connection to the voltmeter remained at room temperature. Measurements were recorded manually. Data acquisition ended when the leads reached 5 K.

A.5 Alligator clip short circuit test

The lengths of the lead wires were twisted together and secured with Kapton tape. The alligator clip connections were clipped together, mounted to the support rod at the same height as the RTD, and slowly lowered into the Dewar. The other ends of the connections were attached to the coaxial, tin-coated copper voltmeter leads at room temperature. Measurements were recorded manually. Data acquisition ended when the leads reached below 20 K.

Appendix B: Further Results

B.1 Short circuit test results

Figure B1. Voltage of short circuit (Twisted leads) along a thermal gradient, polynomial fit

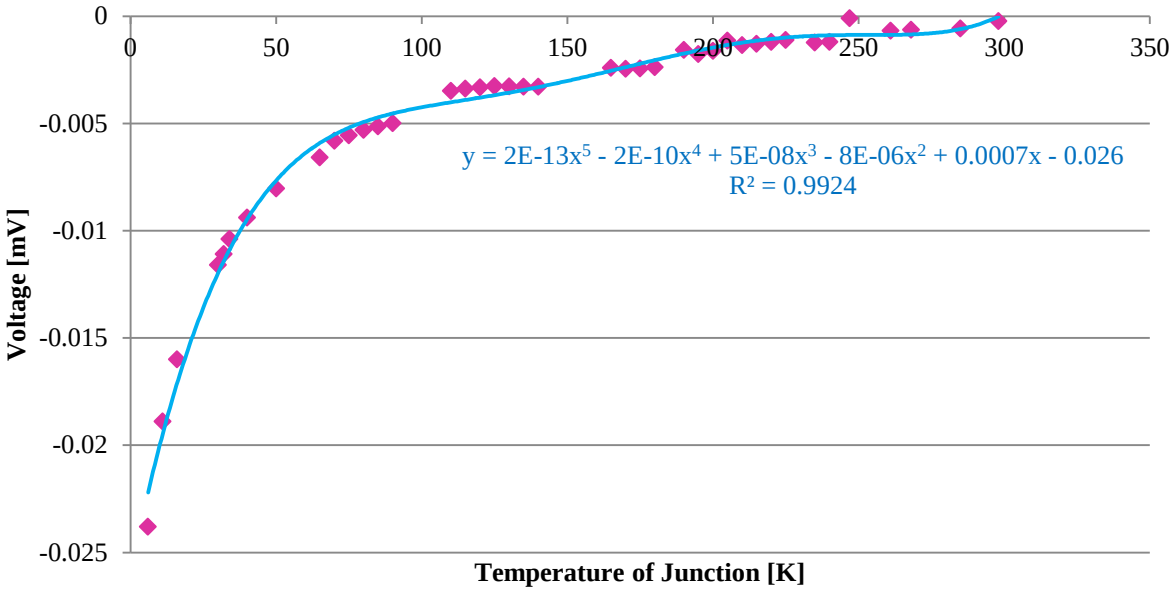

Figure B2. Voltage of short circuit (Alligator clips) along a thermal gradient

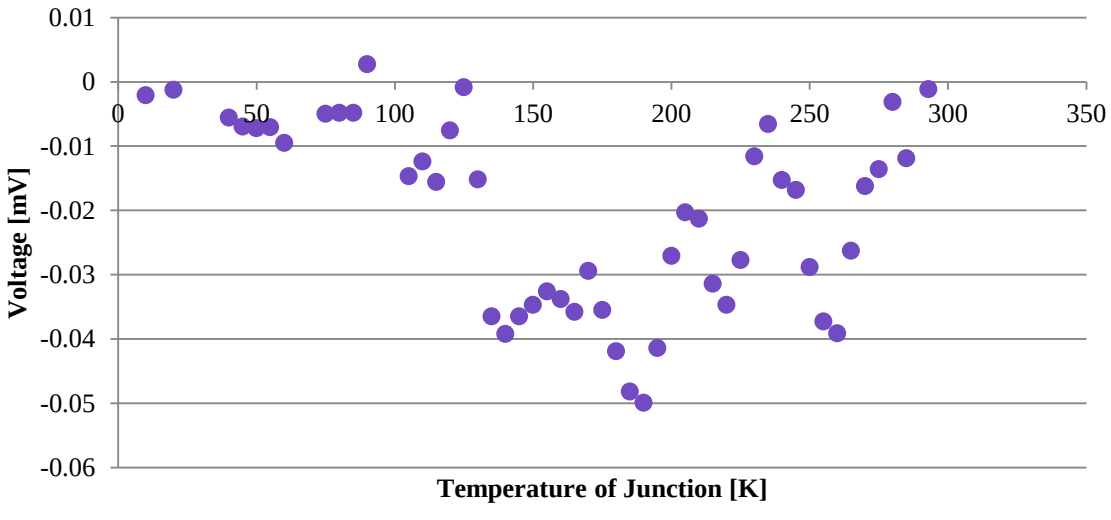

B.2 Theoretical model

Figure B3. Absolute Seebeck coefficients of Nb and Ti vs. temperature with best-fit polynomial models [4]

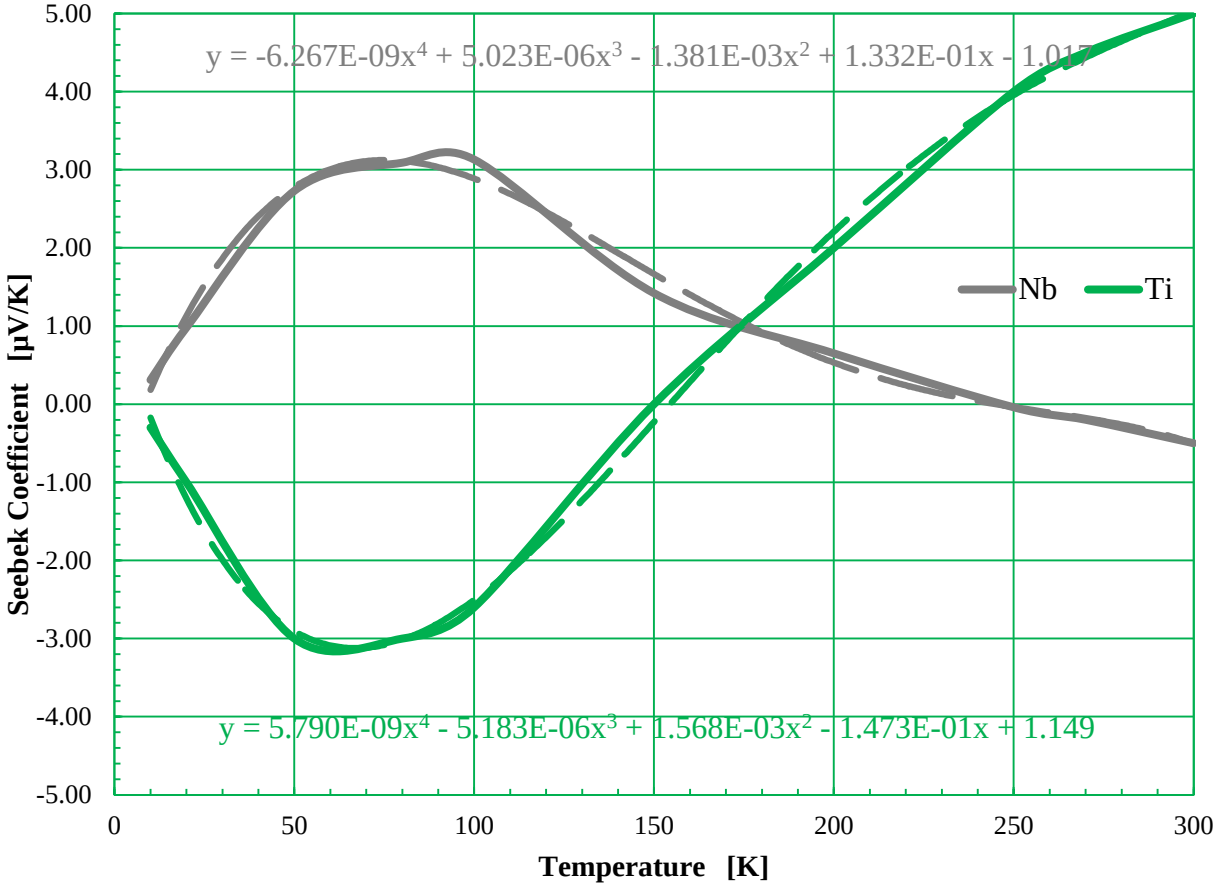

Appendix C: Calculations

C.1 Corrected voltages, experiments 1 and 2

For a Nb+A thermocouple

$$Let\ V_1 = V_{interference} + V_{Nb} - V_A \quad \textbf{(C1)}$$

$$V_2 = V_{interference} + V_A - V_{Nb} \quad \textbf{(C2)}$$

where V_1 is the original voltage and V_2 is the voltage observed when the sources are reversed.

$$\frac{V_1 - V_2}{2} = \frac{V_{interference} + V_{Nb} - V_A - V_{interference} - V_A + V_{Nb}}{2} = V_{Nb} - V_A \quad \textbf{(C3)}$$

Equation (C3) gives the corrected voltage.

C.2 Canceling Seebeck of Copper, experiment 2

Using corrected copper thermocouple voltages,

$$Let\ V_X = V_{Cu} - V_{Nb} \quad \textbf{(C4)}$$

$$V_Y = V_{Cu} - V_A \quad \textbf{(C5)}$$

It follows that

$$V_Y - V_X = V_{Nb} - V_A \quad \textbf{(C6)}$$

Equation (C6) gives the corrected voltage of an Nb+A thermocouple.

C.3 Computing theoretical data

Using best-fit polynomials suited to curves of absolute Seebeck Coefficient, S, vs. temperature, T, for niobium and titanium, it is possible to determine a voltage for a given thermal gradient along the thermocouple. The integral of each curve from 4.2 K to the temperature, T_0, of the thermocouple leads determines the voltage generated by an individual wire; adding these voltages yields the theoretical voltage of the thermocouple circuit as a whole.

Nb best-fit curve:

$Y_1 = -6.267E\text{-}09T^4 + 5.023E\text{-}06T^3 - 1.381E\text{-}03T^2 + 1.332E\text{-}01T - 1.017E$

Ti best-fit curve:

$Y_2 = 5.790E\text{-}09T^4 - 5.183E\text{-}06T^3 + 1.568E\text{-}03T^2 - 1.473E\text{-}01T + 1.149$

Thus

$$V_{tot} = \int_{4.2\ K}^{T_0} Y_1 dT + \int_{4.2\ K}^{T_0} Y_2 dT \quad \textbf{(C7)}$$

where V_{tot} is measured in μV and T_0= 20K, 40K, 60K,…, 300K

C.4 Relating Experimental data to theoretical data

Because the greatest difference in best-fit models between the experimental and theoretical data is in the linear and constant terms, a linear shift is appropriate when determining the relationship between the two data sets. The shift in data increases as junction temperature increases; therefore, it is necessary to calculate a shift factor as a function of temperature. The figures below summarize the determination of such a function.

Table C1 Determining shift in data between theoretical and experimental

Temperature (K)	Theoretical Voltage (mV)	Experimental Average Voltage (mV)	Shift in Voltage (Experimental Average- Theoretical)
4.2	0	-0.0355	-0.0355
10	0.002	-0.0255	-0.0275
20	-0.012	-0.024	-0.0121
40	-0.088	-0.0809	0.00710
60	-0.2	-0.158	0.0413
80	-0.324	-0.240	0.0840
100	-0.441	-0.302	0.139
120	-0.537	-0.339	0.197
140	-0.605	-0.346	0.258
160	-0.643	-0.312	0.331
180	-0.651	-0.235	0.416
200	-0.63	-0.172	0.458
220	-0.586	-0.116	0.469
240	-0.521	-0.0201	0.501
260	-0.442	0.128	0.570
280	-0.35	0.312	0.662
300	-0.246	0.455	0.701

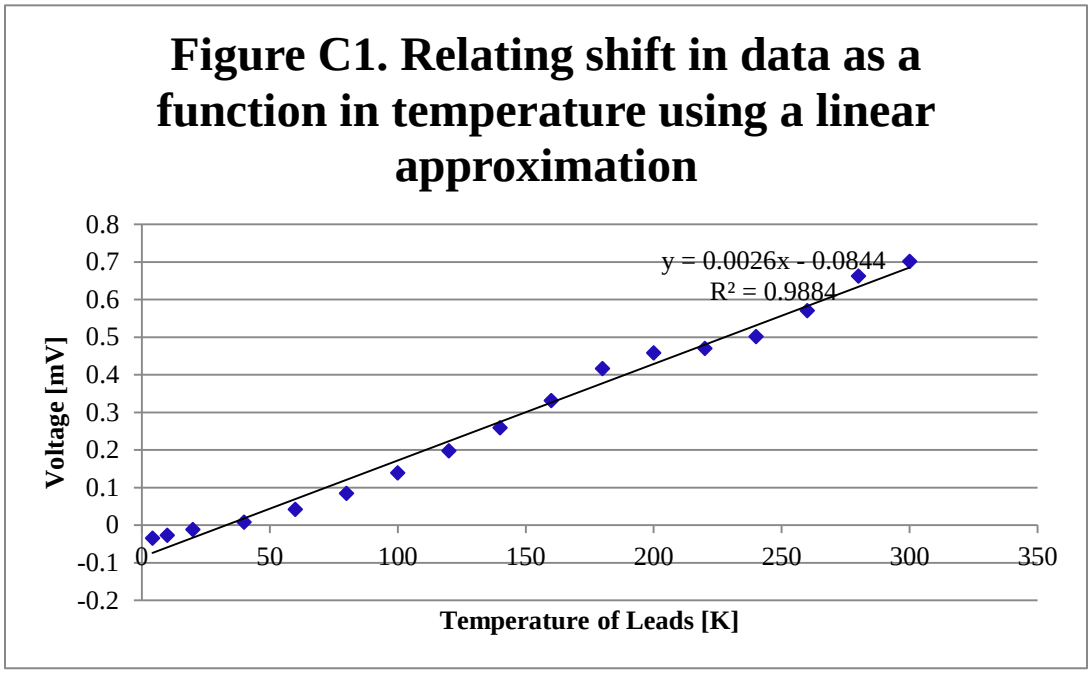

C.5 Uncertainty

As summarized in Tables C2 and C3, uncertainties from the equipment used in the experiments are dominated by uncertainties inherent to the experimental procedure [7,8]. When calculating the uncertainty in the measurements taken, the equipment uncertainties were neglected and only the uncertainties listed in Table 7b were applied. Uncertainties are represented by error bars on Figures 5 and 6 in the Results and Discussion section.

Piece of Equipment	Uncertainty Provided by Manufacturer
Keithley 2182A nanovoltmeter	20±4 ppm
Lakeshore Cernox RTD	0.1%

Table C2 Equipment Uncertainties

Source of Error	Uncertainty Estimate
Distance between leads and RTD	±2K
Background noise in twisted leads	±0.025 mV
Background noise in alligator clip connections	±.0.05mV

Table C3 Uncertainties in Experimental Procedure